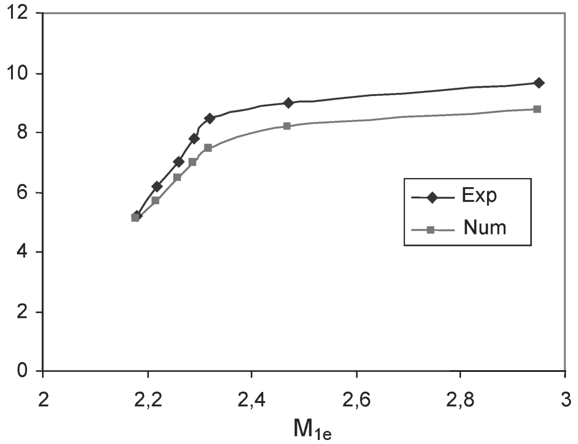

Fig. 5 Evolution of the nondimensional pseudoshock length as a function of the Mach number upstream of the shock M_{1e}.

to approach a constant value for high values of M_{1e} and that L_P extends over 6–15 times the diameter of flow passages for upstream Mach numbers larger than 2.

Conclusions

This Note deals with the study of the shock train structure that appears in the constant-area duct of a supersonic ejector. A CFD model of the airflow inside the ejector has been developed to predict the pressure recovery by pseudoshock. The computational results obtained in the case of the zero-secondary flow configuration of the ejector are in fairly good agreement with experiments. The computational model has demonstrated its capability in accurately capturing the shocks that are formed in the secondary nozzle of the ejector and allows the prediction of the length necessary to fully achieve the pressure recovery. Furthermore, we intend to extend this computational work to more complex flow configurations in ejectors (entrainment of induced flow, choking of the secondary nozzle).

References

[1] Nill, L. D., and Mattick, A. T., "An Experimental Study of Shock Structure in a Normal Shock Train," AIAA Paper 96-0799, Jan. 1996.

[2] Faro, I. D. V., *Handbook of Supersonic Aerodynamics*, Vol. 6, Sec. 17, Bureau of Naval Weapons, NAVWEPS Rept. 1488, Washington, DC, 1964.

[3] Crocco, L., "One-Dimensional Treatment of Steady Gas Dynamics," *Fundamentals of Gas Dynamics*, edited by H. W. Emmons, Princeton Univ. Press, Princeton, NJ, 1958, pp. 110–130.

[4] Matsuo, K., Miyazato, Y., and Kim, H.-D., "Shock Train and Pseudo-Shock Phenomena in Internal Gas Flows," *Progress in Aerospace Sciences*, Vol. 35, No. 1, 1999, pp. 33–100.

[5] Ikui, T., Matsuo, K., and Nagai, M., "The Mechanism of Pseudo-Shock Waves," *Bulletin of the Japan Society of Mechanical Engineers*, Vol. 17, No. 108, 1974, pp. 731–739.

[6] Carrol, B. F., and Dutton, J. C., "Characteristics of Multiple Shock Wave/Turbulent Boundary Layer Interactions in Rectangular Ducts," *Journal of Propulsion and Power*, Vol. 6, No. 2, 1990, pp. 186–193.

[7] Lin, P., Rao, G. V. R., and O' Connor, G. M., "Numerical Analysis of Normal Shock Train in a Constant Area Isolator," AIAA Paper 91-2162, June 1991.

[8] Waltrup, P. J., and Billig, F. S., "Structure of Shock Waves in Cylindrical Ducts," *AIAA Journal*, Vol. 11, No. 10, 1973, pp. 1404–1408.

[9] Sullins, G., and Mc Lafferty, G., "Experimental Results of Shock Trains in Rectangular Ducts," AIAA Paper 92-5103, Dec. 1992.

[10] Mittal, S., and Yadav, S., "Computation of Flows in Supersonic Wind-Tunnels," *Computer Methods in Applied Mechanics and Engineering*, Vol. 191, Nos. 6–7, 2001, pp. 611–634.

[11] Desevaux, P., and Aeschbacher, O., "Numerical and Experimental Flow Visualizations of the Mixing Process Inside an Induced Air Ejector," *International Journal of Turbo and Jet Engines*, Vol. 19, Nos. 1–2, 2002, pp. 71–78.

[12] Desevaux, P., "Analyse Expérimentale du Jet Moteur d'un Éjecteur à Flux Induit Fonctionnant en Régime Mixte," *Journal de Physique 3*, Vol. 4, No. 10, 1994, pp. 1981–1998.

[13] Desevaux, P., Prenel, J. P., and Hostache, G., "Flow Visualization Methods for Investigating an Induced Flow Ejector," *Journal of Flow Visualization and Image Processing*, Vol. 2, No. 1, 1995, pp. 61–74.

[14] Sun, D. W., and Eames, I. W., "Recent Developments in the Design Theories and Applications of Ejectors—A Review," *Journal of the Institute of Energy*, Vol. 68, No. 475, 1995, pp. 65–79.

[15] Fabri, J., and Siestrunck, R., "Supersonic Air Ejectors," *Advances in Applied Mechanics*, edited by H. L. Dryden and T. Von Kármán, Vol. 5, Academic Press, New York, 1958, pp. 1–34.

[16] Robert, C., "Ejecteurs Supersoniques à Flux Induit Nul," Ph.D. Dissertation, l'Université de Franche-Comté, Besançon, France, June 1979.

[17] Matsuo, K., Sasaguchi, K., Tasaki, K., and Mochizuki, H., "Investigation of Supersonic Air Ejectors, Part 1, Performance in the Case of Zero-Secondary Flow," *Bulletin of the Japan Society of Mechanical Engineers*, Vol. 24, No. 198, 1981, pp. 2090–2097.

[18] Desevaux, P., Lanzetta, F., and Bailly, Y., "CFD Modelling of Shock Train Inside a Supersonic Ejector: Validation Against Flow Visualizations and Pressure Measurements in the Case of Zero-Secondary Flow," *Proceedings of the 10th International Symposium on Flow Visualization*, F-0259, Visualization Society of Japan, Kyoto, Japan, 2002.

[19] Desevaux, P., Prenel, J. P., and Jacquet, P., "Static Pressure Measurement Along the Centerline of an Induced Flow Ejector," *Experiments in Fluids*, Vol. 16, Nos. 3–4, 1994, pp. 289–291.

[20] Desevaux, P., "Formation de Nano-Gouttelettes d'Eau au Sein d'un Éjecteur à Air Induit: Une Étude Qualitative par Visualisation de l'Écoulement," *Canadian Journal of Chemical Engineering*, Vol. 79, No. 2, 2001, pp. 273–278.

M. Sichel
Associate Editor

Boundary-Layer Separation in a Turn-Around Duct

V. A. Sandborn*
Colorado State University, Fort Collins, Colorado 80521

Introduction

COMPLEX shear flows are encountered in turbomachinery that may differ from the canonical, two-dimensional boundary layers. The general approach in dealing with such flows is to employ loss coefficients that encompass specific geometries without need for knowledge of the flow details. However, further understanding of the complex flows, such as separation, may allow engineering improvements.

A detailed experimental study of the flow in a small radius of curvature (5-cm) water flow, turn-around duct (TAD) was made[1,2] (Fig. 1). Separation occurs on the inner wall of the duct starting at approximately 150 deg. The very large acceleration of the flow at the entrance to the turn results in a rapid thinning of the layer along the inner wall. Once the flow encounters the adverse pressure gradient at approximately 90 deg, the inner shear layer increases in size and develops very rapidly into a separation bubble that continues around the exit of the turn. Details of the separation bubble shape and size were given by Shin.[2] The present Note examines the mean velocity distributions obtained along the inner surface (tabulated by Shin[2]) at 150, 160, and 170 deg around the turn, as they relate to the separation model. The data were originally taken to aid in the determination of the start of the separation bubble, and so the velocity profiles were not obtained in great detail.

TAD Separation

Laser velocimeter measurements were made in the TAD for duct Reynolds numbers from 2×10^5 to 5×10^5 (Refs. 1 and 2). Typical

Received 8 September 2003; revision received 30 January 2004; accepted for publication 2 February 2004.

*Emeritus Professor, Department of Civil Engineering, Engineering Research Center; v.sandborn@comcast.net. Senior Member AIAA.

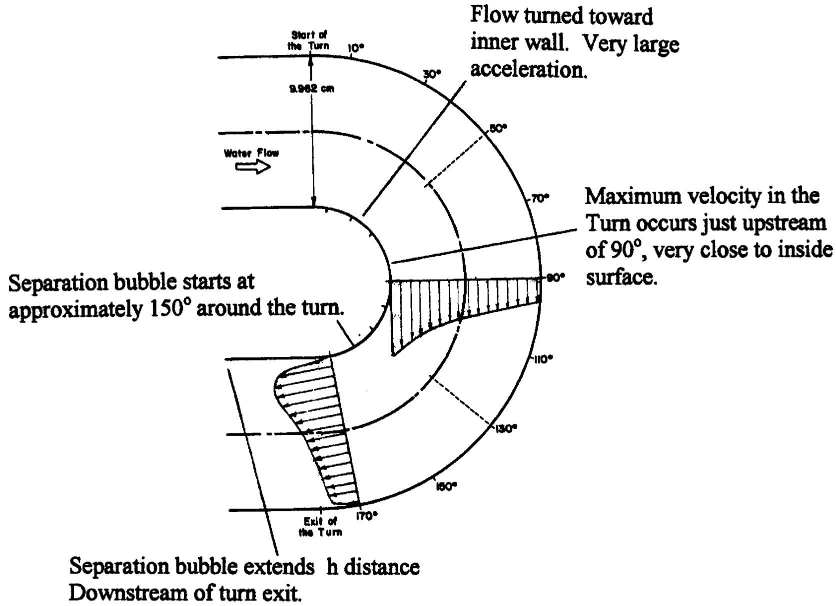

Fig. 1 Flow in the turn-around duct.

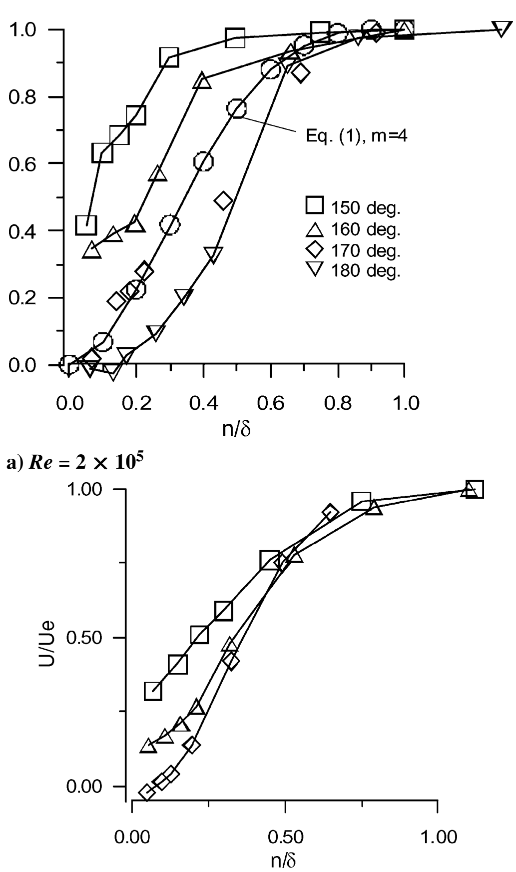

a) $Re = 2 \times 10^5$

b) $Re = 5 \times 10^5$

Fig. 2 Inner surface boundary-layer velocity distribution.

velocity distributions across the duct for $Re = 2 \times 10^5$ are shown in Fig. 1. At 150 deg and beyond, the boundary-layer thickness δ on the inner wall was taken at the point of maximum velocity and was roughly $\delta / h \approx 0.1$ at 160 deg (where h is the duct width). Note that $\delta \approx 1$ cm. The maximum velocity U_e was taken as the outer edge velocity of the inner wall boundary layers. Figure 2 shows the inner wall boundary layers for 150, 160, and 170 deg around the turn, nondimensionalized by δ and U_e. Because the inner wall shear layer thickness was very small, the boundary-layer parameters were computed assuming a simple two-dimensional boundary layer.

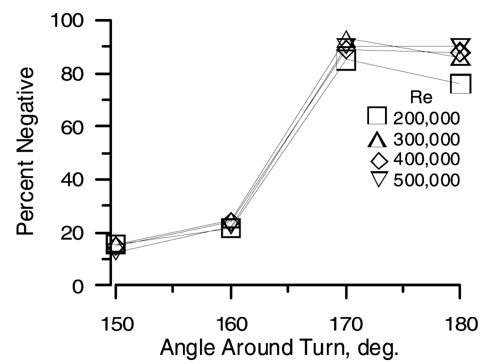

Fig. 3 Extrapolated surface values of the percent flow reversal.

The accuracy of the measurements was limited near the surface due to the diameter of the laser beam (of the order of 0.5 mm). Repeatability of the mean velocity measurements[2] was ± 0.005 m/s. Near the surface in the separation region, the velocity measurements are less accurate due to the reduced sampling rates and the presence of both larger particles and air bubbles. The profile parameters, displacement thickness δ^*, momentum thickness θ, and $H \equiv \delta^* / \theta$ were estimated to be accurate to $\pm 5\%$.

The amount of flow reversal near the surface for the 150-, 160-, and 170-deg locations are shown in Fig. 3. The flow reversal was determined from probability histograms of the laser velocimeter output.

Intermittent transitory detachment (ITD) was defined[3] as the location where the instantaneous backflow occurred 20% of the time. With the exception of the $Re = 2 \times 10^5$ flow, Fig. 3 indicates ITD occurs at approximately the 160-deg location around the turn. The 160-deg location was identified from flow visualization[2] as the location of intermittent separation for the higher-Reynolds-number flows.

Figure 4 is H vs momentum thickness Reynolds number Re_θ for the three locations around the turn. The separation correlations of Sandborn[4] are also noted in Fig. 4. The values of H at 160 deg, excluding the $Re = 2 \times 10^5$ case, fall very close to the intermittent separation correlation. The results (Fig. 4) demonstrate that the extreme shear flow case of the TAD still follows the separation model found for the larger aerodynamic flows. Also shown in the insert of Fig. 4 are the original separation correlations of Sandborn and Kline.[5] As observed,[4] the original Sandborn–Kline correlations appear to be sensitive mainly to the curvature and/or pressure gradient effects on separation.

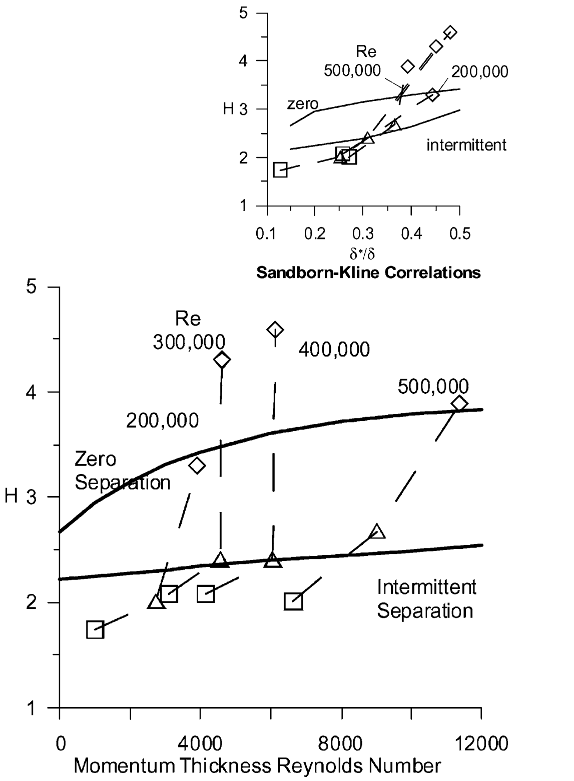

Fig. 4 Comparison of the velocity profile parameters with the separation correlations.

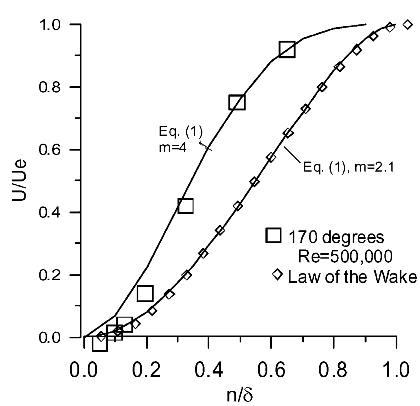

Fig. 5 Mean velocity distributions compared with Eq. (1).

The point of zero-mean surface shear stress separation, $\overline{\tau_w} = 0$, is more of academic interest, although it plays an important role in the development of skin-friction relations[4] and empirical velocity profile representation.

The Sandborn–Kline[5] $\overline{\tau_w} = 0$ correlation was obtained by employing an empirical laminar velocity separation profile,[6]

$$U/U_e = 1 + (1 - y/\delta)^m [m \ln(1 - y/\delta) - 1] \tag{1}$$

Figure 5 shows a comparison of the TAD velocity profile at 170 deg and $Re = 5 \times 10^5$ with Eq. (1) for the case $m = 4$. Equation (1) is also compared with the 170-deg, $Re = 2 \times 10^5$ data in Fig. 2. It was assumed that the normal coordinate n was equivalent to y. The profile (Fig. 5) is beyond the point of $\overline{\tau_w} = 0$; however, the agreement with Eq. (1) for the outer region of the profile $\overline{\tau_w} = 0$ is reasonable. The tabulated law of the wake function,[7] which is found to be one unique case of Eq. (1) for $m = 2.1$, is also shown in Fig. 5. The value of δ for the law of the wake was taken at the point where $U/U_e = 0.995$, which is consistent with the requirements of the measured profiles.[4] Equation (1) can be employed for a wide range of flows and is not limited to large aerodynamic flows.

Conclusions

The velocity distribution in a complex, small radius of curvature, TAD shear flow was shown to follow closely the separation model developed for canonical, two-dimensional, large-Reynolds-number, turbulent boundary layers. The TAD flow produces a very thin shear layer along the inner surface of the initial 90 deg of the turn. Beyond 90 deg, the inner wall shear layer thickens and develops to the start of separation by approximately 150 deg around the turn. The shear layer velocity shape parameters are found to develop through the separation region as predicted by the Sandborn–Kline separation model.

The mean velocity distributions in the region of zero-mean surface shear stress separation were shown to agree with equivalent laminar separation profiles.

References

[1]Sandborn, V. A., and Shin, J. C., "Water Flow Measurements in a 180 Degree Turn-Around-Duct," NASA CR NAS8-36354, 1989.

[2]Shin, J. C., "Experiments on Turbulent Shear Flow in a Turn-Around-Duct," Ph.D. Dissertation, Dept. of Civil Engineering, Colorado State Univ., Fort Collins, CO, Feb. 1990.

[3]Simpson, R. L., "Turbulent Boundary Layer Separation," *Annual Review of Fluid Mechanics,* Vol. 21, 1989, pp. 205–234.

[4]Sandborn, V. A., "Reynolds-Number Correlation for Separation of Turbulent Boundary Layers," *AIAA Journal*, Vol. 41, No. 4, 2003, pp. 744–747.

[5]Sandborn, V. A., and Kline, S. J., "Flow Models in Boundary Layer Stall Inception," *Journal of Basic Engineering*, Ser. D, Vol. 83, No. 3, 1961, pp. 317–327.

[6]Sandborn, V. A., "Equation for the Mean Velocity Distribution of Boundary Layers," NASA Memo 2-5-59E, Feb. 1959.

[7]Coles, D., "The Law of the Wake in the Turbulent Boundary Layer," *Journal of Fluid Mechanics*, Vol. 1, Pt. 2, 1954, pp. 191–226.

A. Plotkin
Associate Editor

Dynamic Motion of Rotating Bunsen Flame Tip in Microgravity

H. Gotoda* and T. Ueda†
Keio University, Yokohama 223-8522, Japan
and
R. K. Cheng‡
Lawrence Berkeley National Laboratory, Berkeley, California 94720

Introduction

MANY combustion phenomena are sensitive to natural convection, and there has been extensive microgravity combustion research on droplet combustion, solid material combustion, or gaseous combustion to elucidate the contributions of buoyancy.[1–3] These studies are mostly performed in drop towers, parabolic aircraft flights, and surrounding rockets. In a Bunsen flame formed under normal gravity, buoyancy-induced instability, that is, flame

Received 17 May 2003; revision received 19 December 2003; accepted for publication 23 January 2004.

*Research Associate, School of Science for Open and Environmental Systems, 3-14-1 Hiyoshi, Kohoku-ku, Kanagawa.

†Professor, School of Science for Open and Environmental Systems, 3-14-1 Hiyoshi, Kohoku-ku, Kanagawa; ueda@mech.keio.ac.jp. Member AIAA.

‡Senior Scientist, Environmental Energy Technologies Division; RKCheng@lbl.gov. Senior Member AIAA.